doi.org/10.1002/hlca.202300150

RESEARCH ARTICLE

HELVETICA chimica acta

Tailoring the Hybridization Density of DNA Biosensors through Tunable Surface Functionalization

Perrine Robin,[a] Lucas Mayoraz,[a] Pauline Skigin,[a] Mounir Mensi,[b] and Sandrine Gerber-Lemaire*[a]

[a] Institute of Chemical Sciences and Engineering, Group for Functionalized Biomaterials, Ecole Polytechnique Fédérale de Lausanne, EPFL SB ISIC SCI-SB-SG, Station 6, CH-1015 Lausanne, Switzerland,
e-mail: sandrine.gerber@epfl.ch
[b] ISIC-XRDSAP, EPFL Valais-Wallis, Rue de l'Industrie 17, CH-1951, Sion, Switzerland

DNA biosensors are promising candidates for the development of point-of-care diagnosis methods. They can be inserted in microfluidic platforms, are often non-expensive, and can be produced for a variety of targeted analytes. However, their development faces several challenges, some of which arise from their surface design. Among the characteristics which affect the binding efficiency of DNA probes to their targeted genes, the packing density and lateral spacing of the probe sequences must be controlled to provide enough binding sites and avoid crowding effect. It has also been demonstrated that increasing the space between the probe and the substrate can enhance the sensitivity of the sensing surface. Herein, we describe a methodology to control the vertical distance between DNA probes and a glass support, and lateral spacing between the probes. Such functionalization strategy could help the development of sensing surface with high hybridization density, and therefore high sensitivity.

Keywords: Biosensors, DNA biosensor, chemical spacer, surface chemistry, surface functionalization, DNA immobilization, glass surface.

Introduction

DNA-based biosensors have recently raised interest for the generation of biomedical detection device. Their low production cost, along with their ability to be miniaturized and customized to any target molecules, make them interesting candidates for point-of-care detection.[1]

To ensure high sensitivity, the immobilization strategy must be carefully designed.[2,3] The effect of the support should also be mitigated, which can be achieved by introducing chemical spacers.[4,5] The insertion of a flexible spacer can also enhance the hybridization capacity of an immobilized oligonucleotide probe.[6] In a previous study, Shchepinov *et al.* investigated the effect of a variety of spacer molecules on the hybridization efficiency of immobilized oligonucleotides on a propylene support. While the presence of charged groups on the spacer molecules had a detrimental effect on the hybridization efficiency, increasing the spacer length resulted in enhanced hybridization performance. In particular, they established that a minimal length of 40 atoms led up to a 150-fold increase in the hybridization efficiency.[4] Another report suggested that increasing the length of the spacer between a DNA probe and a gold surface enhanced the sensitivity of the targeted DNA detection performed through surface-plasmon resonance.[7] A similar conclusion was reported by Lee *et al.*, who studied electrochemical biosensors made of carbon electrodes.[8] Beside controlling the vertical space between the probe and the surface, adjusting the lateral distance between the DNA strands also plays a role in the sensitivity of the sensing surface. Indeed, a maximum of DNA probes should be immobilized on the surface, while keeping enough space in between

Supporting information for this article is available on the WWW under https://doi.org/10.1002/hlca.202300150

to avoid crowding effect and accommodate their targeted genes for hybridization.[2,3,9] In the case of low probe density, the hybridization efficiency (number of probes that can hybridize with their complementary genes) can reach 100% with a fast kinetic. However, for high probe density, the efficiency can drop to 10% and the kinetics are also decreased.[10] For most sensing surfaces, a probe density of 1 to 3 pmol.cm^{-2} is often considered as an optimum.[11] The main strategy to tailor the density of surface-immobilized oligonucleotides includes the variation on the density of binding sites[12–14] or the use of diluent molecules to space the probes from each other.[11,15] While the latter is simple and can be implemented on many type of surfaces, it has been mostly reported on gold electrodes so far.[11,15]

In this work, we present three coating methods involving spacer molecules of various lengths to immobilize DNA probes on glass surfaces. To our knowledge, no study has addressed the incrementation of the spacer length between an immobilized DNA probe and a glass substrate so far. The resulting surfaces were characterized by X-ray Photoelectron Spectroscopy (XPS) and fluorescence assay. A dilution method is also described to tailor the DNA probe density on the substrate while maintaining the spacer length constant. In this work, a SARS-CoV-2 gene was selected as target analyte; however, the functionalization strategies herein presented are independent from the probe sequence and could be implemented for any other oligonucleotide sequence.

Results and Discussion

Three immobilization strategies were investigated on borosilicate sensing slides (**Sen-OH**), as illustrated in *Scheme 1*. The first one, referred as 'Short system', is based on the attachment of DNA through a succinic linker. For the 'Medium system' and 'Long system', tetraethylene glycol (TEG) and polyethylene glycol (PEG) spacers were selected. All coating strategies rely on a silanization step to introduce reactive carboxylic or dibenzocyclooctyne (DIBO) moieties for the 'short' or 'medium'/'long' systems, respectively. For the 'short' system, direct conjugation of amino-modified DNA

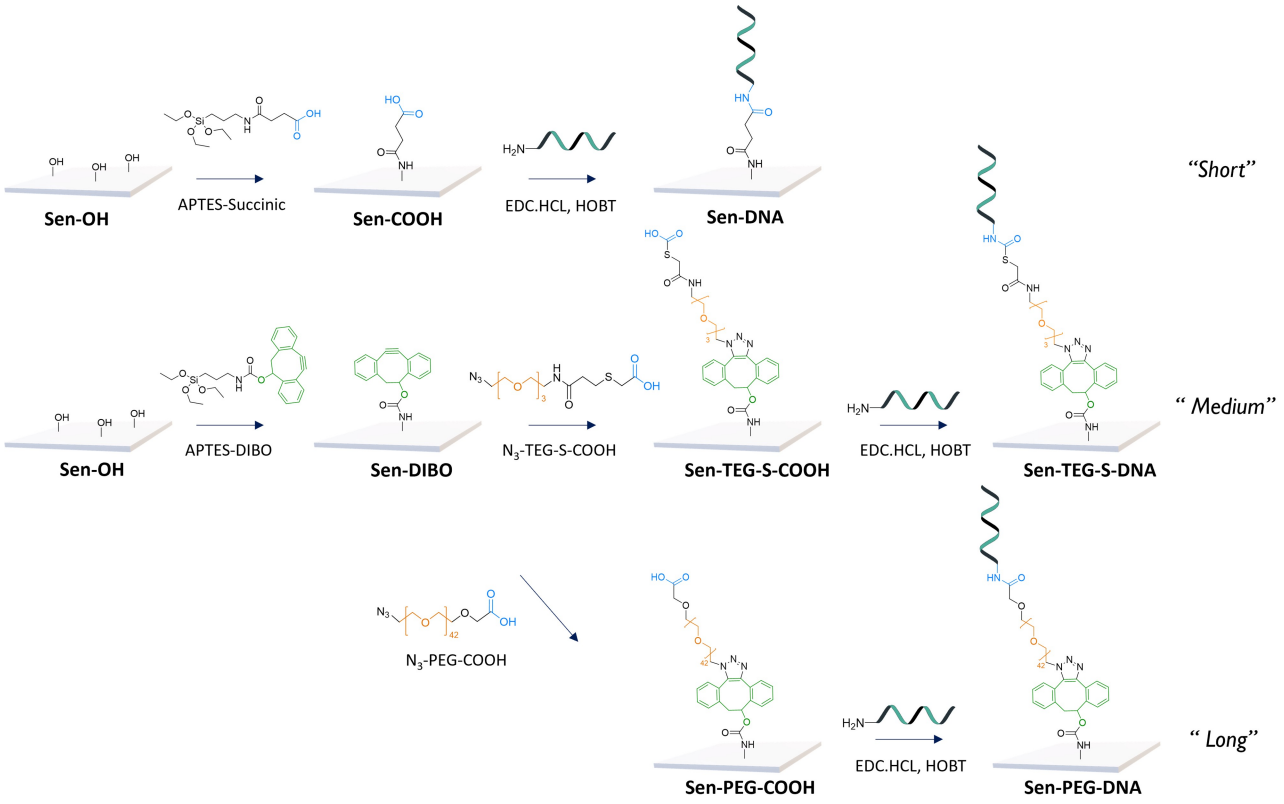

Scheme 1. Overview of the conjugation strategies with three different spacer lengths. Surface silanization was used to introduce reactive carboxylic and DIBO moieties. Medium (TEG) and long (PEG) spacing units were conjugated through SPAAC reactions. Amino-modified DNA probe immobilization was achieved through amide bond formation.

probes was achieved by amide bond formation on the carboxylic acid. For the 'medium' and 'long' systems, the spacing linkers were introduced through strain promoted azide to alkyne [3 + 2] cycloaddition (SPAAC, copper-free click chemistry), using surface DIBO moieties as anchoring sites. The terminal carboxylic acids were later used for covalent conjugation to amino-modified DNA probes.

Synthesis of Spacing Molecules

The silanization reagents **APTES-COOH** and **APTES-DIBO** were prepared from (3-aminopropyl)triethoxysilane (APTES), as detailed in *Supporting Information*, *Section 2.1*. In the case of the 'short' system, the succinic spacer was directly conjugated to (3-aminopropyl)triethoxysilane (APTES) to afford the silanization reagent **APTES-COOH**, as detailed in *Supporting Information*, *Section 2.1*.

The **N_3-TEG-S-COOH** spacer was synthetized from tetraethylene glycol (*Supporting Information*, *Section 2.2*) and was equipped with a sulfur atom among the structure to facilitate the characterization of the modified surface through XPS. The long **N_3-PEG-COOH** spacer, with a molecular weight of 2 kDa, was commercially available.

Overall, the distance from the DNA probes to the surface was respectively of around 1, 3.5 and 22 nm for the 'short' (9 atoms), 'medium' (25 atoms) and 'long' (142 atoms) systems.

Surface Functionalization

Sen-OH slides were activated by plasma treatment (17 min), followed by immersion in a solution of silanization reagents (1 mg/mL) in dry toluene, under inert atmosphere for 48 h. The silanization step was confirmed by XPS, monitoring the apparition of the characteristic peaks (C 1s and N 1s) of the silane derivatives introduced on the resulting **Sen-COOH** and **Sen-DIBO** surfaces (*Figure 1*).

In the case of the **Sen-COOH** surface, the apparition of a shoulder at 288 eV is consistent with the C=O moiety from the carboxylic acids.

The relative intensity of C, N and Si are shown in *Table 1*. The efficiency of the silanization was assessed by the increase in relative C and N content (C/Si and N/Si ratios) from the **Sen-OH** to the modified surfaces. In addition, the N/C ratio matched the theoretical values (1 : 7 = 0.14 for **Sen-COOH** and 1 : 20 = 0.05 for **Sen-DIBO** surfaces). The concordance with theoretical ratios shows that there was no contamination from the atmosphere and that the samples were carefully prepared.

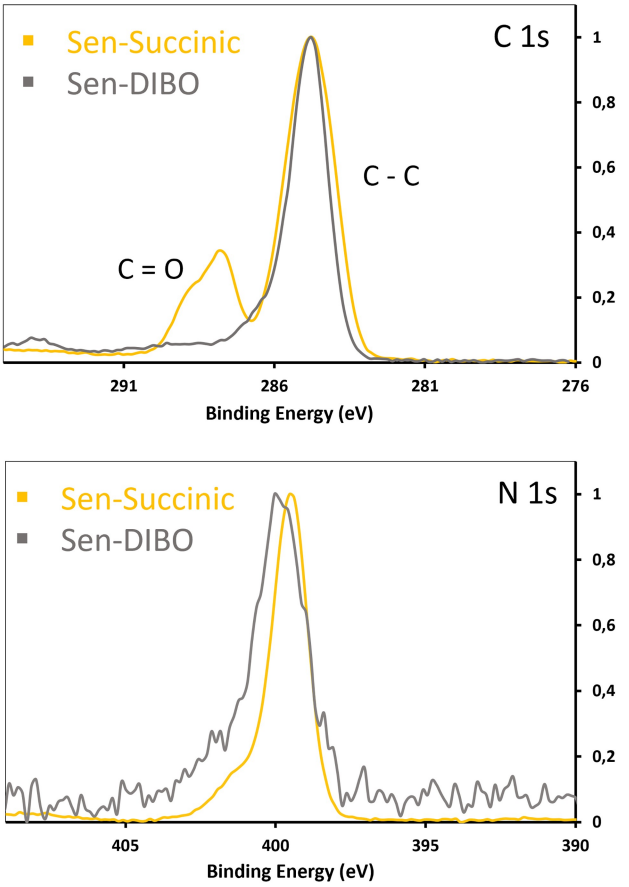

Figure 1. High resolution XPS spectra of C 1s and N 1s scans of **Sen-DIBO** and **Sen-COOH** surfaces.

Table 1. Surface relative atomic concentration of C, N, P, and Si detected through XPS before and after silanization. Surface compositions are expressed as atomic percentage [%].

Surfaces	C 1s %	N 1s %	Si 2p %	C/Si	N/Si	N/C
Sen-OH	22.38	0.81	76.82	0.29	0.01	0.00
Sen-COOH	65.62	9.03	25.35	2.59	0.36	0.14
Sen-DIBO	38.92	1.64	59.26	0.66	0.03	0.04

For the 'medium' and 'long' systems, azido-modified linkers were conjugated to **Sen-DIBO** surfaces by SPAAC reaction, in methanol overnight. XPS analysis of the resulting glass slides showed an increase of C 1s and N 1s signals, as well as the apparition of a S 2p peak in the case of **N_3-TEG-S-COOH**, (see *Supporting information*, *Figure S8*, *Section 3*). XPS spectra of the S 2p signal are shown in *Figure 2*. The signal/noise ratio measured by XPS was low, but coherent with a monolayer coating. A Monte-Carlo simulation was

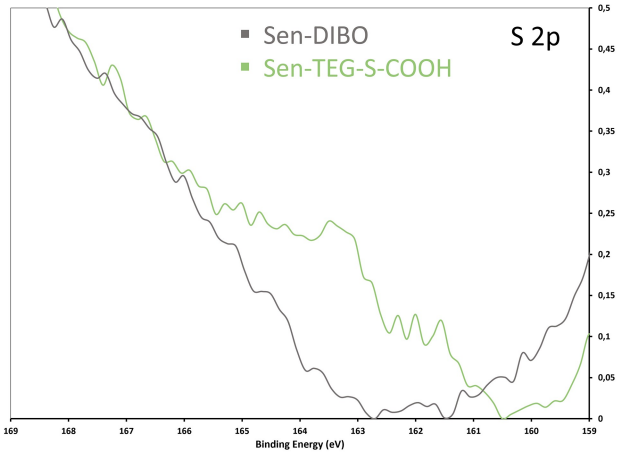

Figure 2. High resolution XPS spectra of S 2p scans of **Sen-DIBO** and **Sen-TEG-S-COOH** surfaces.

performed (*Supporting Information*, *Section 3*, *Table S2*) to confirm the presence of sulfur on the functionalized surfaces.

The relative concentration of C, N, S and Si are given in *Table 2*. The increase of C/Si and N/Si ratios gave evidence for the click conjugation of the **Sen-TEG-S-COOH** and **Sen-PEG-COOH** spacers. Interestingly, the shorter linker resulted in higher increase of the relative C and N content, which may indicate that the SPAAC reaction was more efficient with the **N_3-TEG-S-COOH** than **N_3-PEG-COOH** spacer.

Finally, carboxylic-modified slides were reacted with amino-modified DNA probes using a combination of *N*-(3-dimethylaminopropyl)-*N*-ethylcarbodiimide and 1-hydroxybenzotriazole hydrate (EDC/HOBt) as coupling agent. DNA conjugation was assessed by XPS, monitoring the apparition of a P 2p signal, as shown in *Figure 3*. For the 'long system', the P 2p signal could not be detected by XPS (see *Supporting Information*, *Figure S9*, *Section 3*) as the quantity of DNA probes was likely to be below the limit of detection of the technique. A Monte-Carlo simulation was performed for the P 2p signal (*Supporting Information*, *Section 3*, *Table S3*) to validate the reliability of the detected signal.

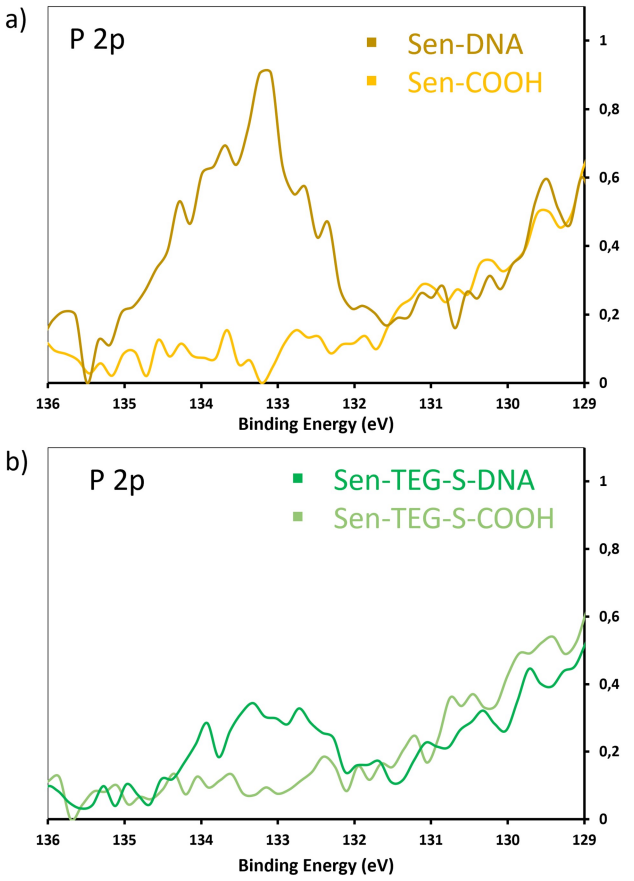

Figure 3. High resolution XPS spectra of P 2p scans of the 'short' (a) and 'medium' (b) systems before and after DNA immobilization.

The elemental composition of DNA-conjugated sensing surfaces is presented in *Table 3*. The detection of P 2p and the evolution of relative C and N content for **Sen-DNA** and **Sen-TEG-S-DNA** surfaces gave evidence for the immobilization of DNA probes on the coated slides. In addition, the intensity of the P 2p signal was lower on the 'medium system' compared to

Table 2. Surface relative atomic concentration of C, N, S and Si detected through XPS before and after click conjugation. Surface compositions are expressed as atomic percentage [%].

Surface	C 1s %	N 1s %	S 2p %	Si 2p %	C/Si	N/Si
Sen-DIBO	38.92	1.64	0.00	59.26	0.66	0.03
Sen-TEG-S-COOH	45.65	3.39	0.70	50.27	0.91	0.07
Sen-PEG-COOH	40.51	1.81	0.00	57.69	0.70	0.03

Table 3. Surface relative atomic concentration of C, N, P and Si detected through XPS after DNA conjugation. Surface compositions are expressed as atomic percentage [%].

Surface	C 1s %	N 1s %	P 2p %	Si 2p %	C/Si	N/Si
Sen-DNA	73.73	12.54	0.15	13.58	5.43	0.92
Sen-TEG-S-DNA	53.07	8.94	0.17	37.82	1.40	0.24
Sen-PEG-DNA	47.92	3.37	0.04	48.67	0.98	0.07

the 'short system', indicating a decrease of DNA probe density with increasing spacer length.

The DNA hybridization density, which corresponds to the amount of probes that are able to hybridize with their targeted gene, was then measured through fluorescence assay following the procedure described in our previous study.[16] Results are presented in *Figure 4*.

As anticipated, the hybridization density obtained at the sensing surfaces varied with the length of the spacer. While the **Sen-DNA** and **Sen-TEG-S-DNA** slides displayed a small variation in hybridization density, respectively 2.18 ± 0.77 and 1.94 ± 0.60 pmol·cm^{-2}, the **Sen-PEG-DNA** surfaces showed a value of only 0.69 ± 0.12 pmol·cm^{-2}. As mentioned above, the efficiency of the SPAAC reaction might be impacted by the elongation of the PEG spacer, thus resulting in a lower density of surface reactive carboxylic groups on **Sen-PEG-COOH** surfaces for conjugation to DNA probes. The length and conformation of the elongated spacer could also decrease the accessibility of carboxylic acid moieties for coupling to the DNA sequence.

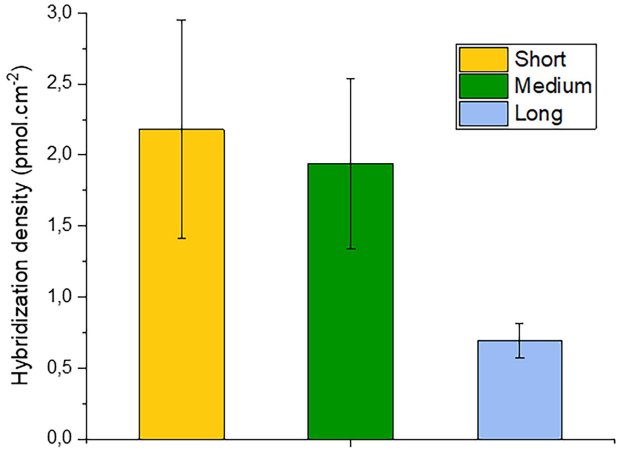

Figure 4. Hybridization density measured at the surface of the 'short', 'medium' and 'long' systems through fluorescence assay. The results are presented as mean values ± SD (3 independent experiments).

Dilution Strategy

To actively tailor the DNA density conjugated at the surface of the glass slides, a dilution method was investigated on the 'medium system', as illustrated in *Scheme 2*. For this purpose, a diluent molecule **N_3-TrEG-OMe** was synthetized from triethyleneglycol (TrEG), that is shorter of one ethylene glycol unit compared to the spacer molecule **N_3-TEG-S-COOH**, and is therefore expected to generate distance around the reactive carboxylic acids. The synthesis of **N_3-TrEG-OMe** is detailed in *Supporting Information*, *Section 2.3*.

Sen-DIBO slides were immersed in mixtures of **N_3-TEG-S-COOH** and **N_3-TrEG-OMe**, in various proportions. The SPAAC reaction was performed overnight at room temperature, in methanol, and the resulting surfaces (**dil-Sen-TEG-S-COOH**) were analyzed by XPS. Monitoring the intensity of the S 2p signal at 163.6 eV (corresponding to C–S–C bonds) showed a clear decrease in S content when increasing the proportion of **N_3-TrEG-OMe** (*Figure 5*). The elemental composition of **dil-Sen-TEG-S-COOH** surfaces and corresponding S/C ratios demonstrated the dilution effect of the TrEG-based diluent, resulting in tunable density of

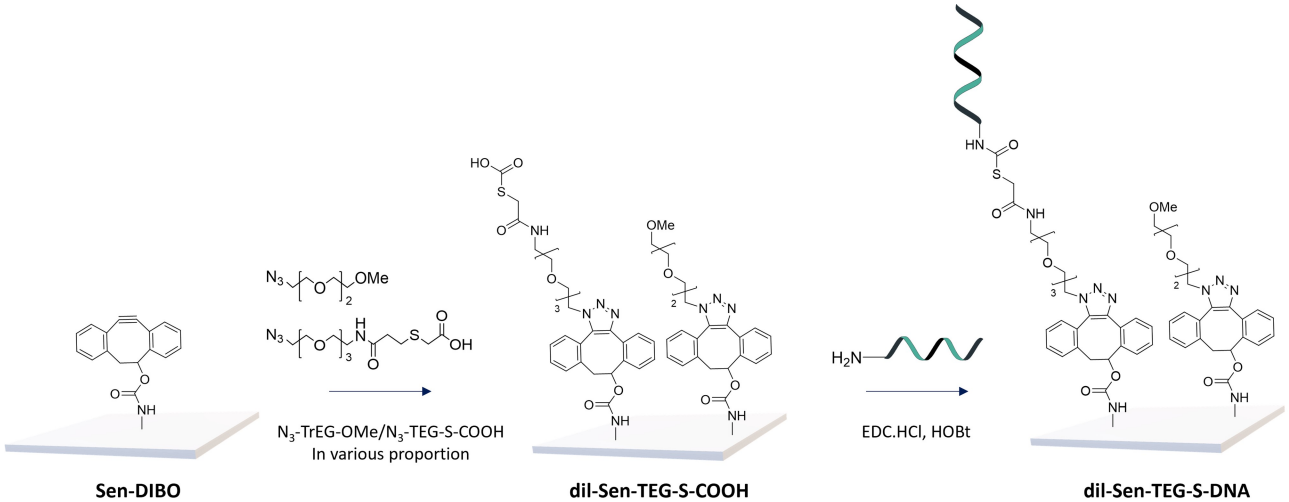

Scheme 2. Dilution method used to tailor the density of DNA probes immobilized at the surface of the 'medium system'.

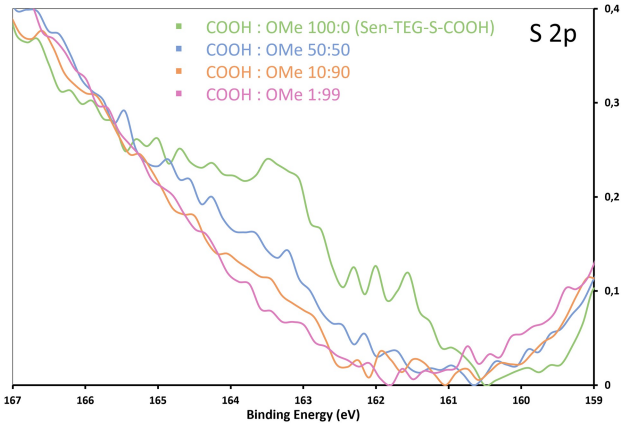

Figure 5. High resolution XPS spectra of S 2p scans of **dil-Sen-TEG-S-COOH** surfaces for different ratios of **N_3-TEG-S-COOH: N_3-TrEG-OMe**. A ratio of 100:0 corresponds to **Sen-TEG-S-COOH** surface.

carboxylic acid moieties for further conjugation to DNA probes (*Table 4*).

Table 4. Surface relative atomic concentration of C, N, S and Si detected through XPS on **dil-Sen-TEG-S-COOH** surfaces. Surface compositions are expressed as atomic percentage [%].

Ratio COOH/OMe	C 1s %	N 1s %	S 2p %	Si 2p %	S/C
100:0[a]	45.65	3.39	0.70	50.27	$1.54{\cdot}10^{-2}$
50:50	39.12	3.85	0.39	56.64	$1.01{\cdot}10^{-2}$
10:90	44.84	3.49	0.31	51.37	$6.94{\cdot}10^{-3}$
1:99	43.07	3.69	0.28	52.96	$6.61{\cdot}10^{-3}$

[a] The ratio 100:0 corresponds to **Sen-TEG-S-COOH** surface.

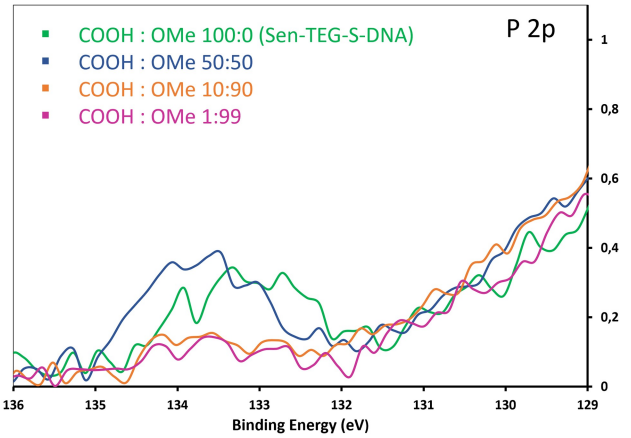

Figure 6. High resolution XPS spectra of P 2p scans of **dil-Sen-TEG-S-DNA** surfaces. A ratio of 100:0 corresponds to **Sen-TEG-S-DNA** surface.

The final functionalization step involved the conjugation of amino-modified DNA probes to **dil-Sen-TEG-S-COOH** slides. The resulting sensing surfaces were analyzed by XPS, recording the spectra of P 2p scans (*Figure 6*) as characteristic signal for the immobilized oligonucleotide sequence (for surface relative atomic concentrations, see *Supporting Information*, *Table S1*). In agreement with the tunable density of surface carboxylic acid moieties, the intensity of the P 2p signal was reduced when increasing the proportion of diluent molecules at the surface. However, the impact of the dilution was moderate for a 50:50 COOH/OMe ratio and became significant for higher proportion of surface TrEG component.

The hybridization density of **dil-Sen-TEG-S-DNA** substrates was quantified using a fluorescence assay, allowing evaluation of the % decrease in hybridization density relative to non-diluted **Sen-TEG-S-DNA** slides (*Figure 7*). In accordance with the XPS data, the hybridization density also decreased when the proportion of the TrEG based diluent increased. At a 50:50 COOH/OMe ratio, we believe that the number of carboxylic acids is already sufficient to obtain a closely packed density of DNA probes, which cannot be further improved due to crowding effect, thus accounting for the close values obtained for 100:0 and 50:50 COOH/OMe ratios.

In this study, the hybridization density was reduced by decreasing the amount of immobilized DNA probes and thus lowering the number of available binding sites. It is to be noted that the reverse effect might be

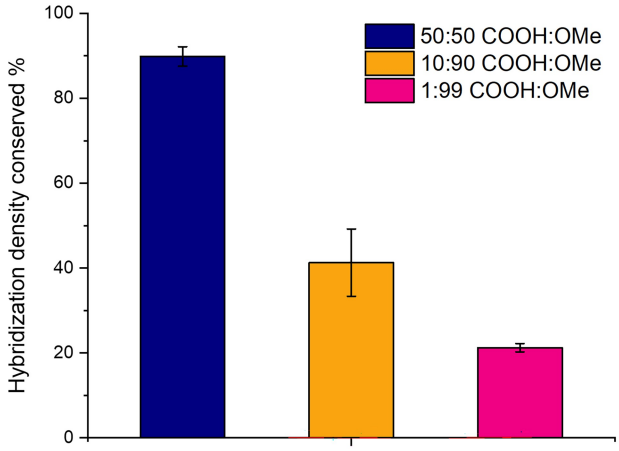

Figure 7. Fraction of the hybridization density conserved upon dilution. The hybridization density measured at the surface of **dil-Sen-TEG-S-DNA** is compared to the one of **Sen-TEG-S-DNA** slides for a same batch. The results are presented as mean values ± SD (three independent experiments).

obtained for other types of biomolecules, especially longer and bulkier targeted genes. Ricci *et al.*, reported that the length and bulk of the targeted genes must be considered when choosing the probe density at the surface of a sensing platform. In most cases, high probe density was giving a higher detection signal, while in the case of a longer and bulkier target, a medium probe density was leading to an increased detection signal compared to the high density surface.[17] Indeed, if the targeted gene is longer than the probe, it might require more space to hybridize, and therefore lead to a higher hybridization density for a surface with a lower probe density. As a result, further investigation should be performed to determine the optimal system to achieve high hybridization density for the detection of long DNA or RNA sequences.

Conclusions

We demonstrated the feasibility of tailoring the probe density and lateral space between DNA probes on glass surfaces for the engineering of DNA-biosensors. The DNA spatial configuration at the surface of sensing platforms is a crucial parameter to consider, as the probe density and lateral spacing can modulate the hybridization efficiency and therefore the ability of the DNA probes to capture their targeted genes in biological samples.

The functionalization strategies relied on a sequence of silanization, followed by click conjugation to spacing molecules and final coupling to amino-modified DNA probes. Based on TEG and PEG backbones, the spacers were equipped with terminal azido and carboxylic acid moieties, for surface immobilization on **Sen-DIBO** slides and conjugation to DNA probes, respectively. The fully covalent 'Short', 'Medium' and 'Long' systems displayed spacer lengths from 9 to 142 atoms between the glass substrate and probe sequence. The DNA density was verified by XPS and the hybridization efficiency was quantified through fluorescence assay, indicating that the probe and hybridization densities both decreased with increasing spacer length.

Then, a dilution method was suggested to tailor the DNA probe density at a constant spacer length, and therefore control the DNA hybridization efficiency of the sensing surfaces. For this purpose, a TrEG-based diluent molecule was added during the click conjugation step, and efficiently decreased the number of carboxylic acids at the surface. Subsequently, both the DNA density and hybridization efficiency at the surface were decreased while increasing the proportion of the diluent molecule.

Experimental Section

Synthesis Procedure

Synthesis of Silanization Reagents. **APTES-DIBO** and **APTES-COOH** were prepared from 3-aminopropyl)triethoxysilane (APTES). Detailed protocols and characterizations are presented in *Supporting Information*, *Section 2.1*.

Analytical Data for **APTES-COOH**. ^{1}H-NMR (400 MHz, $CDCl_3$): 3.85–3.79 (m, 6H, CH_3-CH_2), 3.30–3.24 (m, 2H, CH_2–NH–C=O), 2.70–2.67 (m, 2H, CH_2-CH_2–C=O), 2.53–2.50 (t, 2H, CH_2–CH_2–C=O), 1.68–1.61 (q, 2H, CH_2–CH_2–Si), 1.25–1.21 (t, 9H, 3 × CH_3–CH_2–O–Si), 0.66–0.62 (t, 3H, CH_2–CH_2–Si). HR-ESI/QTOF-MS: 344.150 ($[M+Na]^+$, $C_{13}H_{27}NNaO_6Si^+$; calc. 344.1500), 320.1540 ($[M+H^{-1}]^-$, $C_{13}H_{26}NO_6Si^-$; calc. 320.1535).

Analytical Data for **APTES-DIBO**. ^{1}H-NMR (400 MHz, $CDCl_3$): 7.48–7.46 (d, 1H, 1 × Ar-*H*), 7.35–7.28 (m, 7H, 1 × Ar-*H*), 5.47 (s, 1H, CH_{DIBO}), 3.84–3.83 (q, 6H, CH_3–CH_2–O–Si), 3.21–3.11 (m, 3H, 2 × NH–CH_2–CH_2), 2.92–2.83 (dd, 1H, HC–*H*), 1.66–1.62 (q, 2H, CH_2–CH_2–NH), 1.26–1.17 (m, 9H, 3 × CH_3), 0.67–0.60 (t, 2H, Si–CH_2–CH_2), 490.2031 ($[M+Na]^+$, $C_{26}H_{33}NNaO_5Si^+$; calc. 490.2020).

Spacer Synthesis

N_3-TEG-S-COOH was synthetized from tetraethylene glycol in six steps. A sulfur atom was integrated in the structure to ease the XPS characterization of the modified slides. Detailed protocols and characterizations are presented in *Supporting Information*, *Section 2.2*.

Analytical Data for **N_3-TEG-S-COOH**. ^{1}H-NMR (400 MHz, MeOD): 3.68–3.61 (m, 10H, CH_2–CH_2–O), 3.56–3.54 (t, 2H, CH_2–CH_2–N_3), 3.39–3.36 (m, 4H, CH_2–NH–C=O, CH_2–CH_2–N_3), 3.27 (s, 2H, S–CH_2–C=O), 2.91–2.87 (t, 2H, S–CH_2–CH_2–C=O), 2.54–2.50 (t, 2H, S–CH_2–CH_2–C=O). HR-ESI/QTOF-MS: 387.1313 ($[M+Na]^+$, $C_{13}H_{24}N_4NaO_6S^+$; calc. 387.1309), 363.1339 ($[M+H^{-1}]^-$, $C_{13}H_{23}N_4O_6S^-$; calc. 363.1344).

Diluent Synthesis

N_3-TrEG-OMe was synthetized from triethylene glycol in two steps. Detailed protocols and characterizations are presented in *Supporting Information*, *Section 2.3.* ^{1}H-NMR (400 MHz, $CDCl_3$): 3.69–3.64 (m, 8H, 4 × CH_2–CH_2–O), 3.57–3.54 (m, 2H, CH_2–CH_2–N_3), 3.40–3.37 (m, 5H, Ar–CH_3 and CH_2–N_3). HR–ESI/QTOF-MS: 212.1006 $[M+Na]^+$, $C_7H_{15}N_3NaO_3^+$; calc. 212.1006).

Surface Functionalization

Preparation of **Sen-COOH** *and* **Sen-DIBO** *surfaces.* S-OH slides were exposed to oxygen plasma for 17 min. The substrates were transferred to a glass tube containing a solution of APTES-COOH or APTES-DIBO in anhydrous toluene under nitrogen atmosphere. The slides were incubated for 48 h at 25 °C, washed with toluene, dichloromethane (three times), acetonitrile and methanol.

Preparation of **Sen-TEG-S-COOH** *and* **Sen-PEG-COOH** *surfaces.* **Sen-DIBO** slides were immersed in a solution of **N_3-TEG-S-COOH** or **N_3-PEG-COOH** in dry MeOH (1 mM). The mixture was incubated overnight at 25 °C. The resulting slides were washed with MeOH and MilliQ (3 times each) and used directly for the next step.

Preparation of **dil-Sen-TEG-S-COOH** *Surfaces.* **Sen-DIBO** slides were immersed in a solution of **N_3-TEG-S-COOH**:**N_3-TrEG-OMe** (1 mM total) at various ratio in dry MeOH. The mixture was shaken overnight at 25 °C. The resulting slides were washed with MeOH and MilliQ (three times each) and used directly for the next step.

DNA Immobilization

The procedure was adapted from the protocol reported in our previous study.[16] The carboxylic acid-modified slides (1 cm^2) were immersed in a 2-(*N*-morpholino)ethanesulfonic acid (MES) solution (0.1 M, 2 mL, pH 5) containing EDC·HCl (50 mM) and HOBt (60 mM). A solution of amino-modified DNA probe (5′-NH_2–C6-AACAGCAAGAAGTGCAACGCCAAC) in MiliQ was added (0.1 nmol, 1 μL) and the mixture was incubated overnight at 37 °C, 750 rpm. The slides were then rinsed with Milli-Q water and washed twice with Tween 20 solution (0.1 %, 10 mL), for 10 min. The slides were rinsed with MiliQ and stored in MilliQ at 4 °C until further use.

Surface Characterization

Hybridization Density Evaluation. The procedure was adapted from the protocol reported in our previous study.[16] The DNA-modified surface was immersed in SSC 4X buffer (1.5 mL) to which was added a solution of Cy3-complementary reverse probe (5′-Cy3-GTTGGCGTTGCACTTCTTGCTGTT, 100 μL, 10 μM). The resulting solution was shaken for 1.5 h at 25 °C. After the hybridization step, the surface was rinsed with Milli-Q water and washed with 0.1 % Tween-20 (twice, 10 min, 25 °C), to remove the non-hybridized Cy3-complementary reverse probes. The slide was rinsed with MiliQ (three times), immersed in PBS 0.1 X (2 mL) and heated at 85 °C for 18 min.

The fluorescence of the solution was then measured (λ_{exc} = 532 nm, λ_{em} = 568 nm). The surfaces modified only with carboxylic acids (**Sen-COOH**/**Sen-TEG-S-COOH**/**Sen-PEG-COOH**) were used as negative control.

Supporting Information

The authors have cited additional references within the *Supporting Information*.[18–26]

Author Contribution Statement

Perrine Robin: Conceptualization, Investigation, Methodology, Validation, Data curation, Writing – original draft, Writing – review & editing. Lucas Mayoraz: Investigation, Methodology. Pauline Skigin: Investigation, Methodology. Mounir Mensi: Methodology. Sandrine Gerber-Lemaire: Funding acquisition, Supervision, Project administration, Writing – original draft, Writing – review & editing.

Acknowledgements

The authors thank the technical assistance of the ISIC-NMR platform (ISIC-NMRP, EPFL) and the EPFL mass spectrometry and elemental analysis platform (ISIC-MSEAP, EPFL) for their support with NMR and MS characterizations. The authors also acknowledge the support of Prof. Harm-Anton Klok for plasma activation of **Sen-OH** slides.

This work was funded by the Swiss National Science Foundation (NRP78, Grant n° 4078P0_198265)

and Innosuisse (Innovation project DeMoViS, Grant n° 38934.1 IP-LS).

Data Availability Statement

The data that support the findings of this study are openly available in Zenodo at https://doi.org/10.5281/zenodo.8297556, reference number 8297556.

References

[1] Y. Hua, J. Ma, D. Li, R. Wang, 'DNA-Based Biosensors for the Biochemical Analysis: A Review', *Biosensors* **2022**, *12*, 183.

[2] F. R. R. Teles, L. P. Fonseca, 'Trends in DNA biosensors', *Talanta* **2008**, *77*, 606–623.

[3] S. B. Nimse, K. Song, M. D. Sonawane, D. R. Sayyed, T. Kim, 'Immobilization Techniques for Microarray: Challenges and Applications', *Sensors* **2014**, *14*, 22208–22229.

[4] M. S. Shchepinov, S. C. Case-Green, E. M. Southern, 'Steric Factors Influencing Hybridisation Of Nucleic Acids To Oligonucleotide Arrays', *Nucleic Acids Res.* **1997**, *25*, 1155–1161.

[5] H. Ravan, S. Kashanian, N. Sanadgol, A. Badoei-Dalfard, Z. Karami, 'Strategies for optimizing DNA hybridization on surfaces', *Anal. Biochem.* **2014**, *444*, 41–46.

[6] A. Halperin, A. Buhot, E. B. Zhulina, 'Hybridization at a Surface: The Role of Spacers in DNA Microarrays', *Langmuir* **2006**, *22*, 11290–11304.

[7] S. Peeters, T. Stakenborg, G. Reekmans, W. Laureyn, L. Lagae, A. Van Aerschot, M. Van Ranst, 'Impact of spacers on the hybridization efficiency of mixed self-assembled DNA/alkanethiol films', *Biosens. Bioelectron.* **2008**, *24*, 72–77.

[8] H.-E. Lee, Y. O. Kang, S.-H. Choi, 'Electrochemical-DNA Biosensor Development Based on a Modified Carbon Electrode with Gold Nanoparticles for Influenza A (H1 N1) Detection: Effect of Spacer', *Int. J. Electrochem. Sci.* **2014**, *9*, 6793–6808.

[9] F. Cheng, X. Ma, Q. Feng, H. Wang, M. Yin, W. He, 'Preparation and characterization of DNA array slides via surface Michael addition', *Biointerphases* **2019**, *14*, 061003.

[10] A. W. Peterson, R. J. Heaton, R. M. Georgiadis, 'The effect of surface probe density on DNA hybridization', *Nucleic Acids Res.* **2001**, *29*, 5163–5168.

[11] S. D. Keighley, P. Li, P. Estrela, P. Migliorato, 'Optimization of DNA immobilization on gold electrodes for label-free detection by electrochemical impedance spectroscopy', *Biosens. Bioelectron.* **2008**, *23*, 1291–1297.

[12] K. Miyahara, R. Sakai, M. Hara, T. Maruyama, 'A Cu-free clickable surface with controllable surface density', *Colloid Polym. Sci.* **2019**, *297*, 927–931.

[13] J. Movilli, A. Rozzi, R. Ricciardi, R. Corradini, J. Huskens, 'Control of Probe Density at DNA Biosensor Surfaces Using Poly(L-lysine) with Appended Reactive Groups', *Bioconjugate Chem.* **2018**, *29*, 4110–4118.

[14] S. Chen, M. F. Phillips, F. Cerrina, L. M. Smith, 'Controlling Oligonucleotide Surface Density in Light-Directed DNA Array Fabrication', *Langmuir* **2009**, *25*, 6570–6575.

[15] R. Singh, G. Sumana, R. Verma, S. Sood, M. K. Pandey, R. K. Gupta, B. D. Malhotra, 'DNA biosensor for detection of *Neisseria gonorrhoeae* causing sexually transmitted disease', *J. Biotechnol.* **2010**, *150*, 357–365.

[16] P. Robin, L. Barnabei, S. Marocco, J. Pagnoncelli, D. Nicolis, C. Tarantelli, A. C. Tavilla, R. Robortella, L. Cascione, L. Mayoraz, C. M. A. Journot, M. Mensi, F. Bertoni, I. Stefanini, S. Gerber-Lemaire, 'A DNA biosensors-based microfluidic platform for attomolar real-time detection of unamplified SARS-CoV-2 virus', *Biosens. Bioelectron.: X* **2023**, *13*, 100302.

[17] F. Ricci, R. Y. Lai, A. J. Heeger, K. W. Plaxco, J. J. Sumner, 'Effect of Molecular Crowding on the Response of an Electrochemical DNA Sensor', *Langmuir* **2007**, *23*, 6827–6834.

[18] X. Yan, L. Yang, Q. Wang, 'Lanthanide-Coded Protease-Specific Peptide–Nanoparticle Probes for a Label-Free Multiplex Protease Assay Using Element Mass Spectrometry: A Proof-of-Concept Study', *Angew. Chem. Int. Ed.* **2011**, *50*, 5130–5133.

[19] B. B. Busch, C. L. Staiger, J. M. Stoddard, K. J. Shea, 'Living Polymerization of Sulfur Ylides. Synthesis of Terminally Functionalized and Telechelic Polymethylene', *Macromolecules* **2002**, *35*, 8330–8337.

[20] L. N. Goswami, Z. H. Houston, S. J. Sarma, S. S. Jalisatgi, M. F. Hawthorne, 'Efficient synthesis of diverse heterobifunctionalized clickable oligo(ethylene glycol) linkers: potential applications in bioconjugation and targeted drug delivery', *Org. Biomol. Chem.* **2013**, *11*, 1116–1126.

[21] C. G. Bischak, L. Q. Flagg, K. Yan, T. Rehman, D. W. Davies, R. J. Quezada, J. W. Onorato, C. K. Luscombe, Y. Diao, C.-Z. Li, D. S. Ginger, 'A Reversible Structural Phase Transition by Electrochemically-Driven Ion Injection into a Conjugated Polymer', *J. Am. Chem. Soc.* **2020**, *142*, 7434–7442.

[22] M. E. Jung, A. B. Mossman, M. A. Lyster, 'Direct synthesis of dibenzocyclooctadienes via double ortho Friedel–Crafts alkylation by the use of aldehyde-trimethylsilyl iodide adducts', *J. Org. Chem.* **1978**, *43*, 3698–3701.

[23] M. E. Jung, S. J. Miller, 'Total synthesis of isopavine and intermediates for the preparation of substituted amitriptyline analogs: facile routes to substituted dibenzocyclooctatrienes and dibenzocycloheptatrienes', *J. Am. Chem. Soc.* **1981**, *103*, 1984–1992.

[24] N. E. Mbua, J. Guo, M. A. Wolfert, R. Steet, G.-J. Boons, 'Strain-Promoted Alkyne-Azide Cycloadditions (SPAAC) Reveal New Features of Glycoconjugate Biosynthesis', *ChemBioChem* **2011**, *12*, 1912–1921.

[25] 'Copyright © 2005 Casa Software Ltd', can be found under http://www.casaxps.com/, n.d.

[26] 'Uncertainties in Peak Parameters', can be found under http://www.casaxps.com/help_manual/error_analysis.htm, n.d.

Received August 29, 2023
Accepted November 13, 2023

